Finite element for dynamic analysis of a C-shape piezoelectric actuator

A.N.Mtawa*, W.Mwita
Mbeya Institute of Science and Technology, Mechanical Engineering Department P.O.Box-131, Mbeya, (TANZANIA)
E-mail : alexmtawa@yahoo.com; wamwita2000@yahoo.com
Received: 9th September, 2010 ; Accepted: 19th September, 2010

ABSTRACT

A Finite element model based on the Euler-Bernoulli theory was developed and used to investigate the dynamic behaviour of a C-shape piezoelectric actuator subjected to sinusoidal voltage. The main goal of this study was to develop and validate numerical analysis tools for semicircular shape piezoelectric devices. Once validated for a simple configuration the results can ultimately be extended for more complicated geometries and be helpful in the optimization of the design of curved shape piezoelectric actuators. The dynamic solutions for a free and forced undamped piezoelectric actuator were obtained using a modal analysis method. For the verification of finite element formulation, a MATLAB code was developed to aid in the computation of the fundamental frequency and the corresponding normal mode of a four elements model. The results have been validated by comparing them with published data. The general purpose Finite Element software MSC Marc was also used to simulate the first 3 natural frequencies and their respective mode shapes as well as locating the resonance points for three actuators from three different substrate materials and for three different substrate/Piezoceramic thickness ratios. Results show that an increase of both substrate to piezoceramic thickness ratio and the elastic modulus of the substrate contributed to raise the fundamental frequency of the actuator. It was also found that an actuator with mild steel substrate operated at higher frequencies compared with the aluminium and brass substrates of the same thickness.   © 2011 Trade Science Inc. - INDIA

INTRODUCTION

Smart materials and structures

Smart structures, sometimes referred to as intelligent structures, are structures with extraordinary abilities. They are capable of self-correcting in order to improve and enhance their performance.

A smart structure features a network of sensors and actuators with real-time control capabilities and a host structure (Figure 1).

These sensors and actuators are made from smart materials. This is a group of materials that possess unusual properties. They produce certain responses upon being subjected to certain types of external stimuli such as electrical and magnetic fields, mechanical, chemical and thermal energy. This group of materials includes:
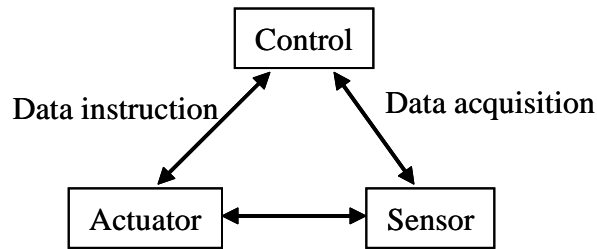
Full Paper

Figure 1 : Basic elements forming a smart structures

Figure 2a : Energy conversion by piezoelectric materials

Piezoelectric (PZT); *Shape Memory Alloys* (SMA), *ElectroRheological* (ER) and *MagnetoRheological* etc.[1,2].

Integration of smart materials in structures is among the most promising technologies for improved reliability of structures and systems. Understanding and control of material properties, geometry and improved control algorithms are among the ultimate objectives of research in this field.

The need and expectation of smart materials for engineering applications have increased enormously, and the expectation of the technology to achieve them is promising. The following are some of the expectations:

- High level of reliability, efficiency and sustainability of structures and systems.
- High security of the infrastructures especially when subjected to extreme and unstructured conditions-Hazard free structures.
- Continuous health and integrity monitoring.
- Damage detection and self-recovery.
- Intelligent operational management system.

Application of smart structures

Examples of potential smart structural systems and some mechanisms are air-craft (monitoring the state of strains in key locations and giving warning to prevent development and propagation of cracks), buildings (earthquake damage resistance, smart windows, electronic windows that sense weather changes and human activity and automatically adjust light and heat), bridges(monitoring of strains, deflections and vibration characteristics in order to warn of impeding failures), ships (hulls and propulsion systems that detect and remove turbulence and prevent deflection), machinery(tools chatter suppression, rotor critical speed control), pipelines(monitoring of leakage and damage in underground pipes of water, oil and gas), medical devices (blood sugar sensors, insulin delivery pumps,
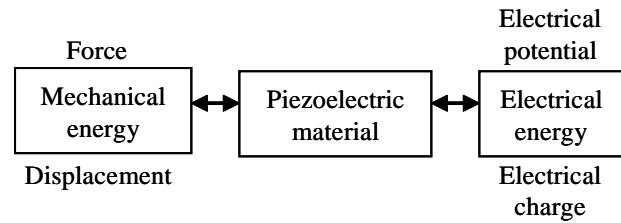
micro-motor capsules that unclog arteries, filters that expand after insertion into vessels to trap blood clots)[1].

Piezoelectric materials

Piezoelectric (PZT), as one of smart materials, undergo mechanical (dimensional or shape) change when subjected to an electric field and vice versa (Figure 2a). This characteristic makes them to be suitable for fabrication of sensors and actuator applications. Energy conversion of piezoelectric devices mainly depends upon the applied voltage, piezoelectric material properties and the geometrical configuration of the actuator or sensor device.

Improvement of actuator performance in terms of displacement, force generation, reduced hysteresis, response time and bandwidth are among the most significant parameters to be studied.

Earlier PZT actuators were mainly used in static operations such as precision positioning or machine, adjustments, but recently PZT actuators are increasingly being demanded for more complicated operations. Dynamically actuated components such as valves and fuel injection devices, together with applications in adaptive smart structures such as shape tuning, vibration excitation, cancellation, and mode shape tuning noise reduction etc, are a few examples. For these operations, fast responses, large displacement and force are issues of concern. In certain applications, particularly in vibration control, small actuators with minimum power consumption, large displacement and force capable of operating both at low and high frequencies are increasingly under demand[3-5].

Curved piezoelectric actuators

Different geometric configurations of piezoelectric sensors and actuators are in use today. Curved piezoelectric actuators are increasingly used nowadays in applications such as vibration control, satellite control etc.
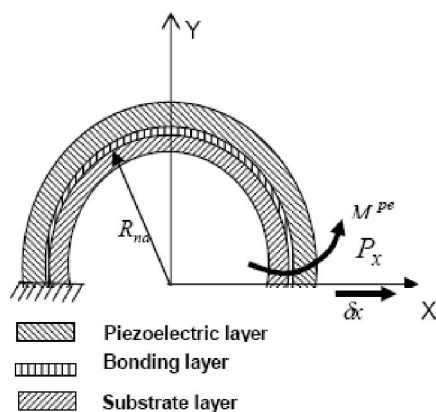
Figure 2b : Unimorph C-shape actuator

A Better understanding of their dynamic behaviour upon application of electric voltage can improve their design and hence effective operation and control of structures[6-8].

There is a wealth of dynamic analysis models developed by J. Moskalik and D. Brei[9] for the C shape actuator configuration, but the focus of their work has been on the analytical (exact) method. The analytical approach is very challenging and involves a huge amount of mathematical work particularly when complicated boundary conditions are involved. The Finite Element Method (FEM) is a widely accepted and powerful tool for analyzing complex structures[10,11]. Also The Finite Element Method lends itself to programming.

The influence of substrate material and the piezoceramic material on the performance of the C actuator as well as the effect of the thickness ratios between the substrate and piezoceramic layers of the actuator under quasistatic condition have been well studied by Mtawa et al.[14,15].

The main focus of this study is to develop a simple computation tool using Finite Element Method to be used to analyze the behavior of the curved shape actuator under dynamic condition.

C-shape piezoelectric actuator

The C-shape piezoelectric actuator, which is a semi-circular (curved) shell, is an invention of A.J. Moskalik and Diann Brei in 1996[12]. When individual C-shape actuators are combined in series and/or parallel it is possible to generate displacement and force larger than a comparable straight bender. The force produced by an array of C- shape actuators is proportional to the number of individual C-shape actuator elements in a parallel arrangement, while the resulting displacement equals the sum of displacements of individual blocks in a series arrangement[13].

A unimorph individual C- shape piezoelectric actuator (Figure 2b) consists of three layers laminated together to form a semicircular shell i.e. one active layer (piezoceramic) and passive layers (bonding and substrate). The piezoceramic (PZT) layer is pre-plated with electrode layers on its inner and outer surfaces. The piezo-ceramic layer together with its electrode is bonded on the outer surface of the substrate. Epoxy is used as the bonding material and a strong bond is created between the piezo layer and the substrate. This ensures that all loads applied by the active layer are transmitted fully to the passive layer. With the unimorph actuator, when the piezoelectric layer expands/contracts in the radial direction the strain in the plane normal to the poling direction (i.e. in the circumferential direction) undergoes a contraction/expansion.

Finite element formulation

Selection/determination of finite elements

The C-shape piezoelectric actuator is obviously a curved shape. For simplicity and for computational economy, flat (straight arc) elements can be used to approximate a curved structure[16,17]. A straight arc element is assumed to undergo both extensional and bending deformations provided that the deformations are small. A straight arc element is obtained by superposing the standard two degrees of freedom (d.o.f) bar element to account for axial displacement with the four d.o.f. beam element to account for lateral and rotational displacements[18] (Figure 3a and 3b). This is partly what contributes to the originality of this paper.

In the present formulation the following assumptions are applied: that the piezoelectric actuator layers are perfectly bonded together (thus continuous strain across the bond is guaranteed, and also shear stresses in the interfaces are ignored. Material behaviour is limited within the linear elastic range (small displacements and strains). The C shape actuator is assumed to be a thin structure/beam, the Euler- Bernoulli model was considered for the finite element analysis of the structure, that is, the effect of transverse shear forces is neglected, cross-sections remain plane and normal to the deformed longitudinal (neutral) axis, the rotational de-
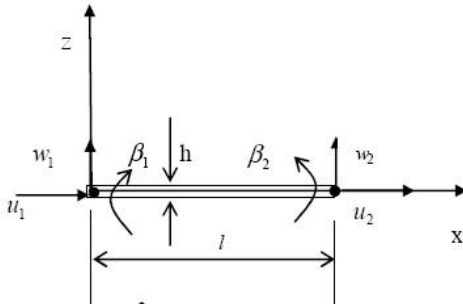
Full Paper

Figure 3a = Straight arc element subjected to both extensional and bending deformations

Figure 3b : Straight arc element assemblage used to model an arc

formation is due to bending alone[19-23].

Kinematics

The model presented in this paper is based on the Euler-Bernoulli theory wherein a multilayered structure is reduced to kinematically equivalent single layer, thereby a 3D problem is reduced to an equivalent 1D problem[24,25]. Each element is bound with two nodes, it consist of the piezoelectric, bonding and substrate layers (Figure 4a and 4b), this means the laminate behaves as a "single" layer with "special" properties.

Each node has three degrees of freedom, that is axial, lateral and rotational displacements. The nodal displacements of the beam element in a local coordinate for an element are given by:

$$(\delta) = \{u_1\ w_1\ \theta_1\ u_2\ w_2\ \theta_2\}^T \tag{1}$$

where u_1, w_1, θ_1 and u_2, w_2, θ_2 are the respective approximate values of the tangential displacement, lateral displacement and rotation at node 1 and node 2 respectively.

The displacement vector $\{D\}$ at any point along the beam at any time may be expressed in terms of the spatial interpolation functions $[N_i]$ and their corresponding nodal degrees of freedom $\{\delta_i\}$ as follows:

$$\{D(x,t)\}=[(N_1(x)), (N_2(x)), (N_3(x)), (N_4(x)), (N_5(x)), (N_6(x))]\{\delta_i(t)\}$$

If the characteristics of the chord may be represented by the corresponding straight arch element with the same cross-section properties as those of the arc, the assumed displacement field equation would be:

$$u(x,t) = a_1(t) + a_2x(t) \tag{2}$$

$$w(x,t) = a_3(t) + a_4x(t) + a_5x^2(t) + a_6x^3(t) \tag{3}$$

These equations can also be rewritten as:

$$U(x,t) = N_1(x)u_1(t) + N_2(x)u_2(t) \tag{4}$$

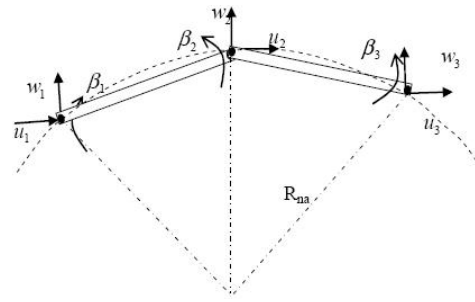$$W(x,t) = N_3(x)w_1(t) + N_4(x)\theta_1(t) + N_5(x)\ w_2(t) + N_6(x)\theta_2(t) \tag{5}$$

Combining equations 4 and 5 we can write:

$$\begin{Bmatrix} u(x,t) \\ w(x,t) \end{Bmatrix} = \{D(x,t)\}$$

$$= \begin{bmatrix} Nu_1(x) & 0 & 0 \\ 0 & Nw_3(x) & Nw_4(x) \\ Nu_2(x) & 0 & 0 \\ 0 & Nw_5(x) & Nw_6(x) \end{bmatrix} \begin{Bmatrix} u_1(t) \\ w_1(t) \\ \theta_1(t) \\ u_2(t) \\ w_2(t) \\ \theta_2(t) \end{Bmatrix} \tag{6}$$

Actuator equations

The general linear piezoelectric actuator for the converse piezoelectric effect can be described in a stress form as follows[26]:

$$\sigma = [Q]^E \{\varepsilon\}-\{\varepsilon\}^T \{E\}$$

$$\sigma = [Q]^E (\{\varepsilon\}-[d]^T \{E\}) \tag{7}$$

where ε = Mechanical Strain, σ = Mechanical stress, d= piezoelectric coupling coefficients for strain- charge form, Q^E = Elastic modulus at fixed electric field, e = piezoelectric coupling coefficients for stress-Charge form, E = Applied electric field and $\{e\}$ = [d][Q]
NB. Superscript T implies matrix transpose.

Strain energy

The strain energy associated with the extension can be given by:

$$U_{ext} = \frac{1}{2}\int_v \{\sigma\}^T \{\varepsilon\} dv \tag{8}$$

From constitutive relationship we can write:

$$U_{ext} = \sum_{p=1}^n \frac{1}{2}\int_0^1 \{\varepsilon_p\}^T Q_p \{\varepsilon_p\} A_p dx \tag{9}$$

where p = 1,2…n is the number of layers. A = the cross-section area. Q = Young's modulus of elasticity
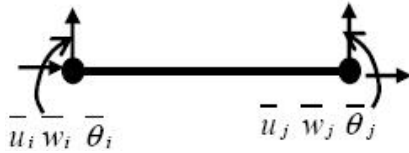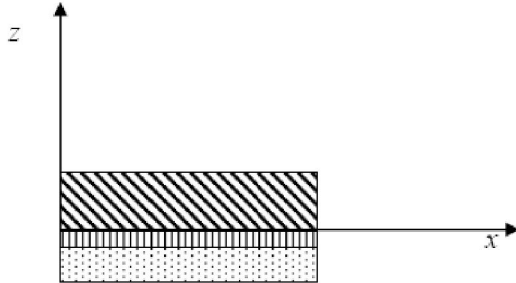
Figure 4a : Straight arc element

Figure 4b : The laminated beam (from bottom to top: substrate, bond and piezoceramic layer)

Eq. (9) can also be written as:

$$U_{ext}(t) = \sum_{p=1}^{n} \frac{1}{2} \int_{0}^{1} [B_{ui}(x)]^T \{\delta_i(t)\}^T Q_p A_p [B_{ui}(x)]\{\delta_i(t)\}dx \qquad (10)$$

where: $[B_u] = \left[\dfrac{\partial N_i(x)}{\partial x}\right]$ represent a matrix giving rela-

tionship between extensional displacement and strain.

The strain energy associated with the bending deformation can be given by:

$$U_{ben} = \sum_{p=1}^{n} \int_{0}^{1} \frac{M^2}{2Q_p I_p} dx \qquad (11)$$

But from mechanics of materials, the bending moment is given by

$$M = QI \frac{d^2 w}{dx^2} \qquad (12)$$

where Q and I are the Young's modulus of the material and the second moment of area of a cross section about the neutral axis respectively.

Substituting equation 12 into equation 11 and after some rearrangement, the instantaneous strain energy due to bending becomes:

$$U_{ben}(t) = \sum_{p=1}^{n} \int_{0}^{1} \left[\frac{d^2 w(t)}{dx^2}\right]^T \frac{Q_p I_p}{2} \left[\frac{d_2 w(t)}{dx^2}\right] dx$$

$$= \sum_{p=1}^{n} \int_{0}^{1} [B_w(x)]^T \{\delta_i(t)\}^T \frac{Q_p I_p}{2} [B_2(x)][\delta_i(t)]dx \qquad (13)$$

But $B_w = \left[\dfrac{\partial N_i x)}{\partial x}\right]$ is the matrix describing the re-

lationship between lateral displacement and the bending strain.

Strain energy related to piezoelectric induced strain can be calculated using the following equation:

$$U_{pe} = \int_{ve} \frac{1}{2} \{\sigma\}^T [Q]^{-1} \{\sigma\}^T dv \qquad (14)$$

Substituting eq. (7) into eq. (14) we obtain:

$$
\begin{aligned}
U_{pe} &= \frac{1}{2} \int_{ve} \left(\frac{\{[Q_{pe}](\{\varepsilon\} - [d]^T\{E_z\})\}^T}{[Q_{pe}]^{-1}[Q_{pe}](\{\varepsilon\} - [d]^T\{E_z\})} \right) dv \\
&= \frac{1}{2} Q_{pe} b t_{p} \int_{0}^{1} [B(x)]^T \{\delta_i(t)\}^T [B(x)]\{\delta_i(t)\}dx - \\
&\quad Q_{pe} b t_p \int_{0}^{1} [B(x)]^T \{\delta_i(t)\}^T d_{31} E_z dx + \\
&\quad Q_{pe} b t_p \int_{0}^{1} E_z^2 d_{31}^2 dx
\end{aligned}
\qquad (15)
$$

The total strain energy for the actuator is now given by the summation of bending, extension and induced piezoelectric strains:

$$U = U_{ext} + U_{ben} + U_{pe}$$

$$U = \frac{1}{2}\{\delta(t)\}^T [k_e]\{\delta(t)\} - Q_p d_{31} E_z b \, t_p$$

$$\int_{0}^{1} [B(x)]^T \{\delta(t)^T dx + Q b t_p \int_{0}^{1} E_z^2 d_{31}^2 dx \qquad (16)$$

where: $[k_e]$ = Stiffness matrix of an element in a local coordinate system given by,

$$[k_e] = \sum_{i=1}^{n} \int_{0}^{1} \left(\frac{[B_{ui}(x)]^T Q_p A_p [B_{ui}(x)] +}{[B_{wi}(x)]^T Q_p I_p [B_{wi}(x)]} \right) dx \qquad (17)$$

The elemental stiffness in a global reference system becomes:

$$K_e = [\psi]^T [k_e][\psi] \qquad (18)$$

where ψ = Transformation matrix given by,

$$\psi = \begin{bmatrix} q_i & -r_i & 0 & 0 & 0 & 0 \\ r_i & q_i & 0 & 0 & 0 & 0 \\ 0 & 0 & 1 & 0 & 0 & 0 \\ 0 & 0 & 0 & q_i & -r_i & 0 \\ 0 & 0 & 0 & r_i & q_i & 0 \\ 0 & 0 & 0 & 0 & 0 & 1 \end{bmatrix} \qquad (19)$$

where $q_i = \cos\beta_i$ and $r_i = \sin\beta_i$. β_i is an angle defining orientation of the ith element with respect to global co-

Full Paper

ordinate system.

Kinetic energy

The kinetic energy of an element is given by:

$$T(t) = \frac{1}{2} \sum_{p=1}^{n} \int_{0}^{L} \rho_p \, A_p \left[\left(\frac{\partial u_i(x,t)}{\partial t} \right)^2 + \left(\frac{\partial w_i(x,t)}{\partial t} \right)^2 \right] dx \quad (20)$$

where ρ_p is the mass density per unit length of the pth layer. A_p The cross section area of the pth layer.

Taking into consideration the assumption that there is a perfect bond between the layers, it implies that all points on the actuator cross-section will move with the same velocities in the respective directions. The kinetic energy of an element eq. (20) becomes:

$$T(t) = \frac{1}{2} \left\{ \dot{D} \right\}^T \int_{0}^{1} \rho_p A_p \left(\begin{array}{c} [N_{ui}(x)]^T [N_{ui}(x)] + \\ [N_{wi}(x)]^T \left\{ \dot{D} \right\}^T [N_{wi}(x)] \end{array} \right) dx$$

$$\left\{ \{\dot{D}\}^T [m_e] \{\dot{D}\} \delta \right\} \quad (21)$$

where, $[m_e]$ =Is a local mass matrix of an element given by,

$$[m_e] = \sum_{p=1}^{n} \int_{0}^{1} \rho_p A_p [N]^T [N] dx \quad (22)$$

where N= shape functions (eq.6)

Similarly, using transformation matrix (eq. 19), the elemental global mass matrix becomes:

$$[M_e] = [\psi]^T [m_e] [\psi] \quad (23)$$

The elemental mass and stiffness matrices are then combined to obtain their respective global mass and stiffness matrices [M] and [k] of the entire structure (actuator) while the boundary conditions are imposed.

$$[M] = \sum_{e=1}^{Ne} [\Psi]^T [M_e] [\Psi] \quad (24a)$$

$$[K] = \sum_{e=1}^{Ne} \Psi^T [K_e] [\Psi] \quad (24b)$$

where N_e is the number of elements in the entire structure (actuator).

Equations of motion

Equations of motion that governs the dynamic response of the structure can be derived by requiring the work of external forces to be equal to the work of internal, inertia and viscous damping forces for any small motion that satisfies both compatibility and essential boundary conditions(admissibility)[17]. Assuming no externally applied mechanical load for a single element the equation of motion becomes[27-29].

$$M_e \ddot{D} + C_{D_e} \dot{D} + K_e D = P_e \quad (25)$$

where: M_e and K_e are global mass and stiffness matrices of an element respectively.

$\ddot{D}$ = A vector of nodal accelerations

$\dot{D}$ = A vector of nodal velocities

D = A vector of nodal displacements

C_D = A matrix containing viscous damping terms.

P_e = Piezoelectric load vector given by

$$P_e = Qbt_{pe}d_{31}E_z \int_{0}^{1} [B]^T dx \quad (26a)$$

$$P_e = Qbt_{pe} d_{31} E(-1 \, 0 \, a \, 1 \, 0 \, -a)^T$$
$$= \{-F \, 0 \, M \, F \, 0 \, -M\}^T \quad (26b)$$

Assuming $E = \dfrac{V_2 - V_1}{t_{pe}} = \dfrac{V}{t_{pe}}$ and $v_1 = 0$ then

$$F = \pm Qbd_{31}V \quad (27a)$$
$$M = \pm aQbd_{31}V \quad (27b)$$

F and M are the induced actuator force and bending moment respectively. a = Moment arm (a distance from the neutral axis to the midline of the piezoceramic layer). t_{pe} represent the thickness of the piezoceramic layer.

If the continuity at the inter-element nodes is imposed then the induced piezoelectric force and moments are assumed to be applied at the free end tip of the piezoelectric layer. This is due to the fact that there will be force cancellations at these nodes.

Eq. (25) represents the dynamic behaviour of an element. If equations of motion of all elements are assembled and then followed by applying the appropriate boundary conditions it yields the equation of motion of the entire C-shape piezoelectric actuator.

Eq. (25) can be rewritten into the forced vibration equation by assuming the displacements, forces, and actuator voltages are harmonic variables with different frequencies. If the right hand side is put equal to zero the equation is then reduced to the eigenvalue problem. From which eigenvalues ω_i and the eigenvectors (u_i, w_i and θ_i) can be determined.

Frequency response analysis

Modal analysis method

The amplitude – frequency response problem can

be solved using the modal analysis method. In this method the expansion theorem is used where the displacements of masses are expressed as a linear combination of the normal modes of the system. Assuming that the system response is governed by 'm' modes of vibration, a set of 'm' uncoupled differential equations of second order is obtained. A solution of theses equations is equivalent to the solutions of equations of 'm' single degrees of freedom[30].

The solution of equation 25 using modal analysis becomes,

$$D(t) = X^{(1)}q_1(t) + X^{(2)}q_2(t) + ... + X^{(n)}q_n(t) = \sum_{i=1}^{n} X^{(i)}q_i(t)$$

(28)

where $X = X^{(1)}, X^{(2)}, ... X^{(n)}$ is the normal mode matrix

and $q(t) = \begin{Bmatrix} q_1(t) \\ q_2(t) \\ ... \\ q_3(t) \end{Bmatrix}$ are the time-dependent generalized

(modal) coordinates,

The nodal acceleration in terms of generalized coordinates becomes,

$$\ddot{D}(t) = X\ddot{q}(t)$$

(29)

Substituting eq. (29) into eq. (25) we obtain,

$$MX\ddot{q}(t) + K Xq(t) + C_D X\dot{q}(t) = P(t)$$

(30a)

Multiplying eq. (30a) by X^T both sides,

$$X^T MX\ddot{q}(t) + X^T KXq(t) + X^T C_D X\dot{q}(t) = X^T P(t)$$

$$\overline{M}\ddot{q}(t) + \overline{K}q(t) + \overline{C}_D\dot{q}(t) = Q(t)$$

(30b)

where: $\overline{M} = X^T M X$ = the generalized modal mass matrix, $\overline{K} = X^T KX$ = the generalized modal stiffness matrix, $\overline{C}_D = X^T C_D X$ = the generalized modal damping matrix.
$Q(t) = X^T P(t)$ = the generalized forces

Writing $\overline{C}_d = 2\lambda_i \omega_i^2$, where λ_i is a modal damping factor, and if the modal vectors are normalized in such a way that

$$\overline{M} = X^{(i)T}MX^{(i)} = \begin{cases} 0 \text{ for } i \neq j \\ 1 \text{ for } i = j \end{cases} \equiv I = diag(1)$$

where I is the identity matrix, and

$$\overline{K} = X^{(i)T}KX^{(i)} = \begin{cases} 0 \text{ for } i \neq j \\ \omega_i^2 \text{ for } i = j \end{cases} = diag(\omega_i^2)$$

where ω_i is the eigenfrequency of the ith mode, then eq. (7.29b) reduces to a set of decoupled equations of motion given by,

$$\ddot{q}(t) + \omega^2 q(t) + 2\lambda\omega^2 \dot{q}(t) = Q(t)$$

(31)

Eq. (31) is a non homogeneous differential equation which ordinary methods can now be used to solve for individual responses in the modal coordinate system.

The ith decoupled equation of motion will be,

$$\ddot{q}_i(t) + \omega_i^2 q_i(t) + 2\lambda_i \omega_i^2 \dot{q}_i(t) = Q(t)$$

(32)

Modal solution

Eq. (32) has the same form as those describing the dynamic response of a damped single degree of freedom harmonic oscillator whose complete solution is given by,

$$q_i(t) = e^{-\lambda_i \omega_i t}\left\{\cos \omega_{di}t + \frac{\lambda_i}{(1-\lambda_i^2)^{0.5}}\sin \omega_{di}t\right\}qi(0)$$

$$+ \left\{\frac{1}{\omega_{di}}e^{-\lambda_i \omega_i t}\sin \omega_{di}t\right\}\dot{q}(0) +$$

$$\frac{1}{\omega_{di}}\int_0^t Q_i(\tau)e - \lambda_i\omega_i(t-\tau)\sin \omega_{di}(t-\tau)d\tau$$

(33)

$i = 1, 2, ...n$

where $\omega_{di} = \omega i\sqrt{1-\lambda_i^2}$ is a damped frequency.

$q_i 0$ and φ_i are constants (generalized displacements and phase angles respectively) which must be defined from the modal initial conditions.

$$q_i 0 = \frac{Q_i 0}{\omega_i^2 \sqrt{\left[\left\{1-\left(\frac{\Omega}{\omega_i}\right)^2\right\} + \left(2\lambda_i \frac{\Omega}{\omega_i}\right)^2\right]}}$$

(34a)

$$\varphi i = \tan^{-1}\left\{\frac{2\lambda_i \frac{\Omega}{\omega_i}}{1-\left(\frac{\Omega}{\omega_i}\right)^2}\right\}$$

(34b)

Full Paper

TABLE 1 : Material properties and dimensions

Property and unit	PZT26	Aluminium	Brass	Mild steel	Epoxy
External radius[mm]	10	8.82	8.82	8.82	9.0
Thickness[mm]	1	0.25, 0.31, 0.5,1.0,2.0	0.25, 0.31, 0.5,1.0, 2.0	0.25, 0.31, 0.5,1.0, 2.0	0.18
Length[mm]	10	10	10	10	10
Piezoelectric strain coefficient d_{31} [m/v]	-1.3e-12	0	0	0	0
Elastic modulus $\dfrac{N}{m^2}$	76e09	7.0e10	1.10e11	1.90e11	5.2e09
Density (kg/m^3)	7.8e03	2.7e03	8.56e03	7.85e03	1.90e03
Maximum Voltage[VAC/mm]	200	-	-	-	-

TABLE 2 : Electromechanical properties of the PZ6

Properties	Value	Unit
s_{11}^E	$1.30e^{-11}$	
s_{12}^E	$-4.35e^{-12}$	
$s_{13}^E = s_{23}^E$	$-7.05e^{-12}$	$\dfrac{m^2}{N}$
$s_{44}^E = s_{55}^E$	$3.32e^{-11}$	
s_{66}^E	$3.47e^{-11}$	
d_{31}	$-1.28e^{-10}$	
d_{32}	$3.28e^{-10}$	$\dfrac{C}{N}$
d_{15}	$3.27e^{-10}$	
ξ_{11}^σ, r	1190	
ξ_{22}^σ, r	1190	
ξ_{33}^σ, r	1330	

Relative value to vacuum permittivity $\xi_o = 8.85 \times 10^{-12} \dfrac{F}{m}$

For i = 1, 2, ……n, is the number of degrees of freedom
where Ω = the driving frequency.

The modal solutions obtained from eq. (33) are then transformed back to obtain the solutions in the physical coordinates by using relationship (29).

Eigenvalue problem

In order to solve the equation of motion (eq. 25) using the modal analysis method it is necessary first to solve the eigenvalue problem.

The natural frequencies ω_i and the respective modes of vibration $X^{(i)}$ of the piezoelectric actuator are obtained from the nth order polynomial in ω^2 by using eq. (25) by assuming an undamped free vibration condition i.e. all external mechanical and electric excitations are assumed to be zero. This yields an eigenvalue problem of the form:
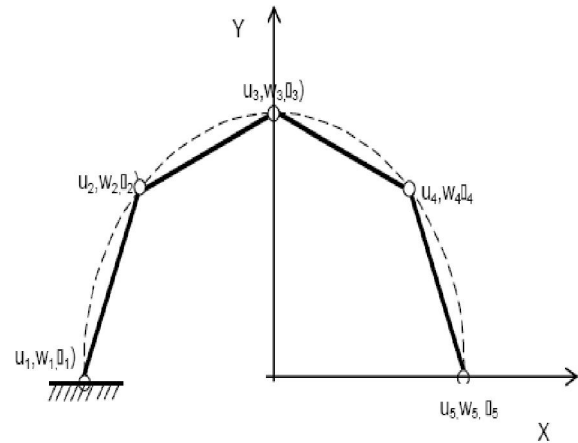

Figure 5 : C-shape piezoelectric actuator approximated with four straight arc elements

$$\det(-\omega_2 M + K) = 0 \qquad (35)$$

The corresponding eigenvectors can be obtained by applying the following equation,

$$(-w_i^2 M + K)X^{(i)} = 0, \text{ for } i = 1, 2, ……n \qquad (36)$$

NUMERICAL EXAMPLES

Computation of eigen frequency with the aid of MATLAB

In order to verify the validity of the finite element formulation the dynamic solution for a free/forced piezoelectric actuator under sinusoidal excitation was obtained using the modal analysis method. The curved actuator was approximated (divided) into 4 equal elements (Figure 5). With the fixed-free boundary conditions, the local and global stiffness and mass matrices for each element (eq. 17, 18, 22, 23) and later for the whole structure (eq. 24a, 24b) were determined. The material and geometrical characteristics of a C-shape piezoelectric actuator used in the analysis are shown in TABLE 1.

The 3 lowest natural frequencies for the actuators with aluminium, brass and mild steel substrates each of three different thicknesses were computed with the aid of MATLAB code developed for this purpose. The results were compared to those calculated using the experimentally validated formula (eq. 37) obtained from reference[9]. The results show good agreement as indicated in figure 6a-8a. An error of approximately 1.4% was noted. Their corresponding frequency-amplitude response curves are shown in figure 6b-8b.
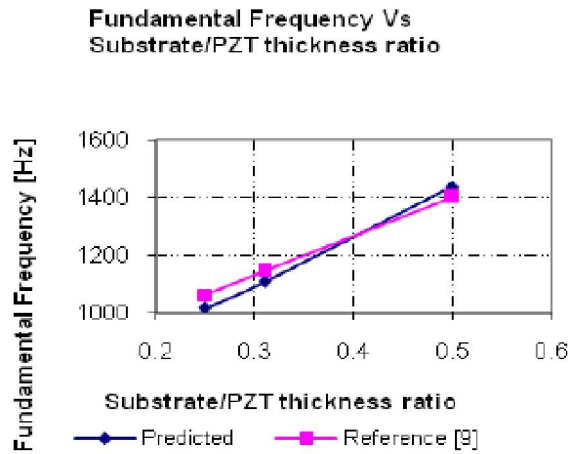
Full Paper

Figure 6a : Comparison of values of fundamental frequency for aluminium substrate
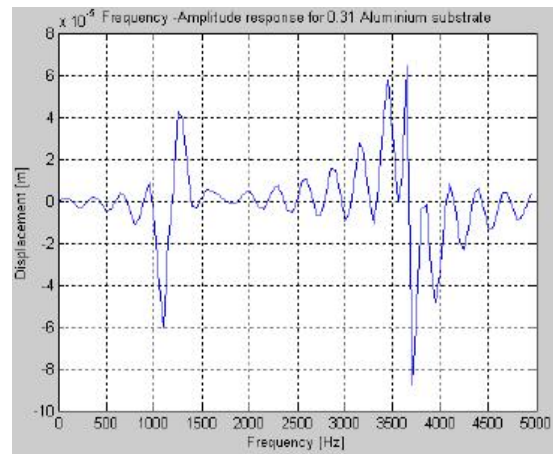

Figure 6b : Frequency - response curves for aluminium substrate at an excitation voltage of 10V, damping coefficient = 0.707
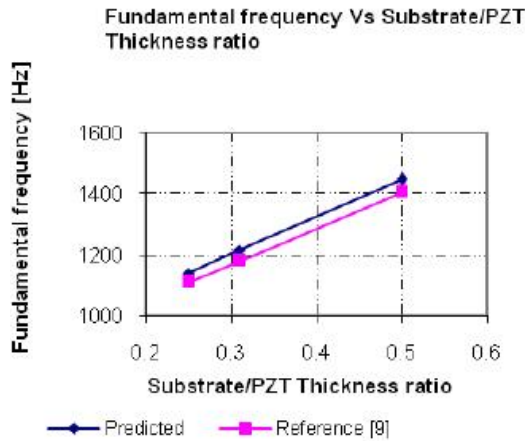

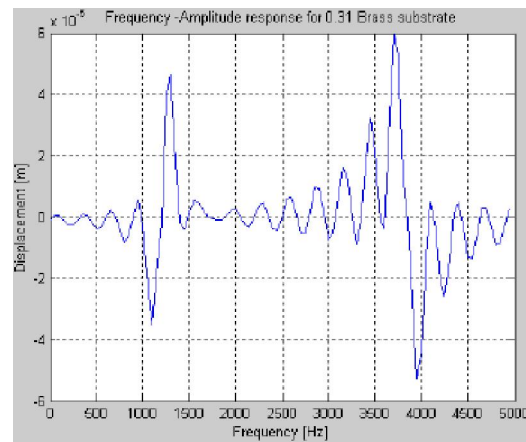**Figure 7a : Comparison of values of fundamental frequency for brass substrate**

Figure7b : Frequency-response curves for brass substrate, (excitation voltage=10V, damping coefficient =0.7071)

$$\left(\omega_i^2 = \frac{D\lambda_i^2}{\rho R_{na}^4} \right) \quad (37)$$

where $\omega_i = i^{th}$ Natural frequency, $D =$ Composite bending stiffness[Nm²], $\lambda_i = i^{th}$ Non- dimensional natural frequency, $\rho =$ mass per length [kg/m] and $R_{na} =$ Radius of neutral axis[m]

Dynamic analysis simulation using MSC aarc

Overview

A dynamic modal analysis was performed to obtain the resonance modes of the actuator, and then a harmonic analysis was performed to determine the dynamic response of the actuator to an alternating voltage. Displacements at a range of frequencies around resonance points were determined. The dimensions and material data for the models used in the simulation are as shown in TABLE 1 and 2.

Resonance points for the C-shape piezoelectric actuator for 3 different substrate materials (i.e. Aluminium, Brass and Mild Steel) were determined. For each material three thicknesses (i.e. 0.25mm, 0.31mm, and 0.5mm) were analysed.

Boundary conditions

One electrode was placed on one node on the inner surface of the piezoelectric ceramic to serve as ground terminal, while another electrode was placed on one node at the outer surface of piezoelectric ceramic to serve the live terminal. In the model, these electrodes are made by tying the potential degree of freedom of all nodes belonging to the respective surface to one node, that is all nodes on the inner surface are tied up to the ground terminal while the outer surface nodes are tied up to the live terminal.

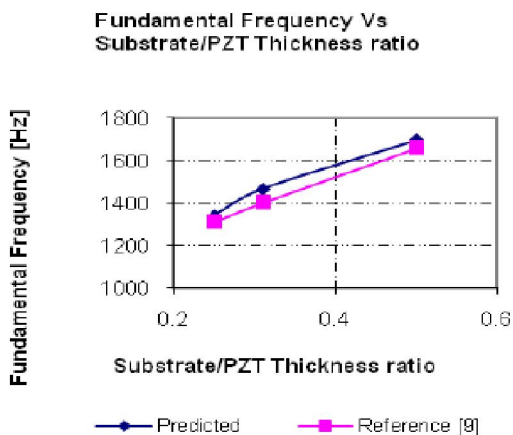The left end tip was fixed while the right hand one

Full Paper

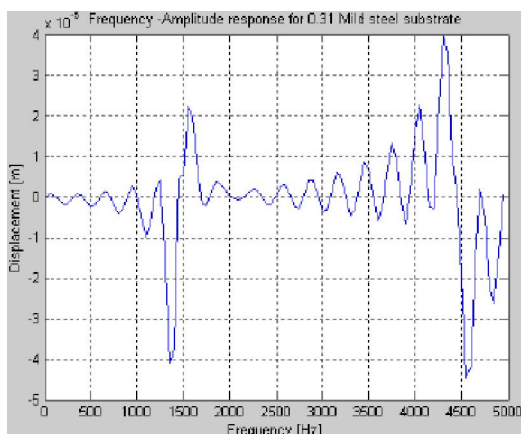**Figure 8a : Comparison of values of fundamental frequency for mild steel substrate**

Figure 8b : Frequency-response curves for a mild steel substrate (excitation voltage=10V, damping coefficient =0.7071)

was left free to oscillate. Plane stress element type 160 was used for the piezoelectric material. This element is mechanically equivalent to element 3 which was used for the substrate materials. This element type has three degrees of freedom; the first two are for the X_ and Y_ displacement, and the third is for the electric potential.

Modal analysis

Load cases and piezoelectric dynamic modal parameters set to search for eigenfrequencies were as follows:

The LANCZOS method was used, whereas a number of frequencies were set to 3. The frequencies obtained are shown in figure 9-11 (appendix B).

Harmonic analysis

For the harmonic analysis, the same model built for modal analysis was used. A new load case was set to suit harmonic boundary conditions. The frequency range was

selected to be around the first 2 natural frequencies, i.e. from 1 kHz and 5 kHz into 50 steps. Results obtained are shown in figure 12 through 14(Appendix B).

Figure 12 for example, shows the X-displacement at frequencies 1053 Hz and 3276Hz which is close to the first two resonant frequencies. The tip displacement magnitude along the frequency range is plotted to show the static solution (i.e. 0.676 Micrometer) at 0 Hz, and the resonance around the first and second natural frequencies.

For both modal and harmonic analysis simulation a 0.25mm substrate was used.

RESULTS AND DISCUSSION

Finite element models based on Euler Bernoulli beam theory were used to perform the dynamic analysis of C-shape actuator consisting of a three layer unimorph laminated beam (Piezoceramic layer, adhesive layer and metallic substrate) where the only deformation impetus was an actuation strain induced in the piezoelectric layer.

The Effect of thickness and substrate material on the displacement and on the operating bandwidth is as shown in figure 6b-8b for a 0.31mm substrates and figure 12-14 (appendix B) for 0.25mm substrates. The results show that an increase of both substrate/PZT thickness ratio and the elastic modulus of the substrate contribute to raise the fundamental frequency of the C-shape actuator. This implies that with appropriate combination of the thickness ratio and the elastic properties of the actuator it can be possible to determine the location of the fundamental frequency and thus set the range over which the actuator can operate before reaching resonance frequency. From the results obtained it can also be concluded that an actuator with a mild steel substrate can operate at higher frequencies compared to aluminium and brass substrates of the same thickness.

It can also be noted that, in this study the C- actuator was approximated using one dimensional curved actuator and more importantly only 4 finite elements (Straight arc) were used. The results reported in section 5.1 indicate that the predicted results and the results calculated using eq. (37) from reference[9] give an error of approximately 1.4%. This is apparent that if
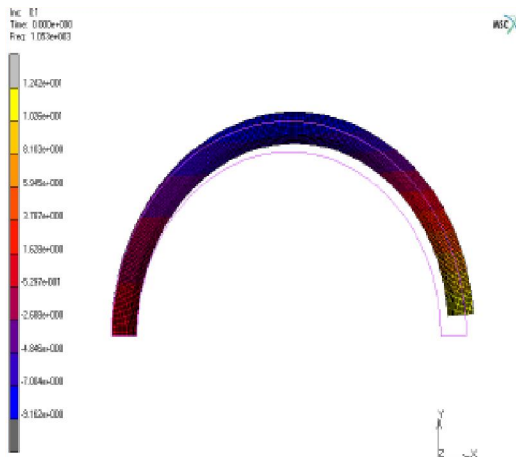
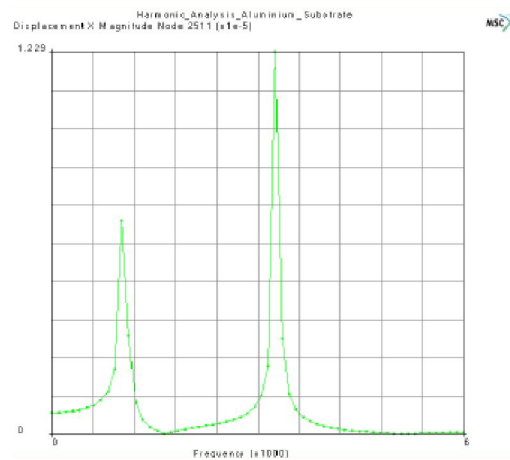**Figure 9 : First Mode shape for a 0.25mm Aluminium substrate**

Figure 12 : the first two resonance points for a 0.25mm Aluminium substrate (i.e. at 1053 and 3276 Hz respectively)
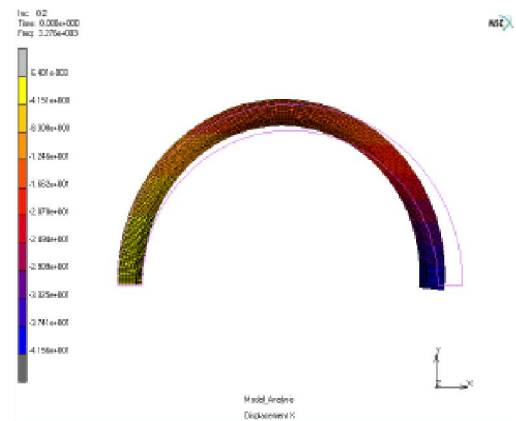

Figure 10 : Second Mode shape for a 0.25mm Aluminium substrate
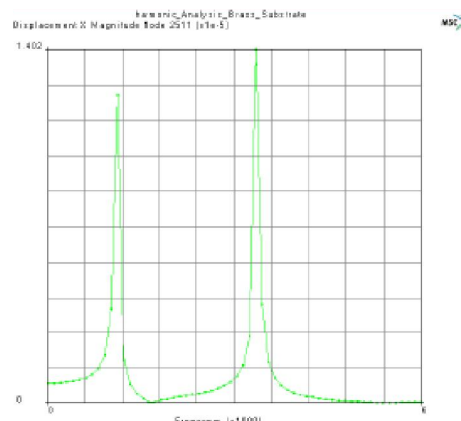

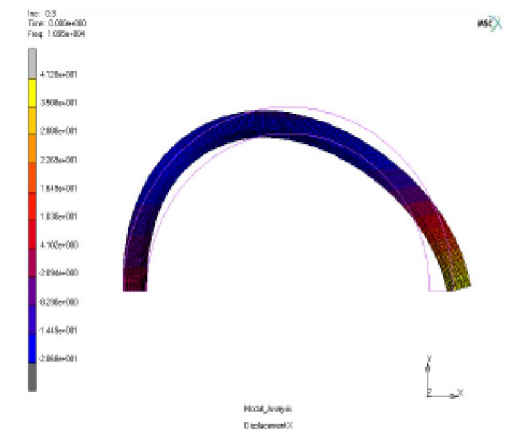**Figure 13 : The first two resonance points for a 0.25mm mild steel substrate (i.e. at 1100and 3360 Hz respectively)**

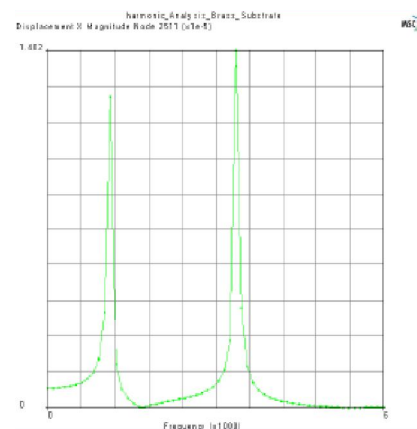**Figure 11 : The third mode shape for a 0.25mm Aluminium substrate**

Figure 14 : The first two resonance points for a 0.25mm brass substrate

the number of elements is increased much more accurate results could have been obtained. In view of this, it can be concluded that the simplicity of the model can remarkably reduce the computational time.

ACKNOWLEDGEMENT

Full Paper

of Smart Materials and Structures laboratory at Cape Peninsula University of Technology- South Africa, for his guidance, advice and for allowing most of the work to be done in the laboratory.

REFERENCES

- [1] A.V.Srinivasan, D.McFarland, Michael; Cambridge: Cambridge University Press, 'Smart Structures Analysis and Design', **(2001)**.
- [2] M.V.Andhi, B.S.Thomson; Michigan State University, 'Smart Materials and Structures', **(1992)**.
- [3] Christopher Niezrecki, Diann Brei, Sivakumar Balakrishanan, Andrew Moskalik; 'Piezoelectric Actuation', State of the Art, The Shock and Vibration Digest, **33(4)**, 269-280 **(2001)**.
- [4] N.J.Conway, Sang-Gook Kim; Technical Digest, 454-457 **(2004)**.
- [5] E.V.Ardelean, D.G.Cole, R.L.Clark; Journal of Intelligent Material Systems and Structures, **15**, 879-889 **(2004)**.
- [6] El Mostafa Sekouri, Yan-Ru Hu, Anh Dung Ngo; Mechatronics, **14**, 1007-1020 **(2004)**.
- [7] You-Di Kuang, Guo-Qing Li1, Chuan-Yao Chen; Smart Mater.Struct., **15**, 869-876 **(2006)**.
- [8] J.M.Han, T.A.Adriaens, Willem L.de Koning, Reinder Banning; Modeling Piezoelectric Actuators IEEE/ASME Transactions on Mechatronics, **5(4)**, 331 **(2000)**.
- [9] J.Moskalik, D.Brei; Journal of Sound and Vibration, **243(2)**, 317-346 **(2001)**.
- [10] Young-Hun Lim, Vasundara V.Varadan, Vijay K.Varadan; Smart Mater.Struct., **6**, 161-168 **(1997)**.
- [11] S.X.Xu, T.S.Koko; Finite Elements in Analysis and Design, **40**, 241-262 **(2004)**.
- [12] A.J.Moskalik, Diann Brei; Journal of Intelligent Material Systems and Structures, **3**, 577-587 **(1997)**.
- [13] A.J.Moskalik, Diann Brei; Smart Structure and Materials, **8**, 531-543 **(1999)**.
- [14] A.N.Mtawa, B.Sun, J.Gryzagoridis; Journal of Smart Materials and Structures, **16**, 1036-1042 **(2007)**.
- [15] A.N.Mtawa, B.Sun, J.Gryzagoridis; Journal of Sensors and Actuators A, **141**, 173-181 **(2008)**.
- [16] Fumio Kikuchi; Journal of Computer Methods in Applied Mechanics and Engineering, **5**, 253-276 **(1975)**.
- [17] D.R.Cooks, D.S.Malkus, M.E.Plesha; 'Concepts and Applications of Finite Element Analysis', New York, John Wiley & Sons, 345 **(1989)**.
- [18] K.M.Liew, X.Q.He, M.J.Tan, H.K.Lim; International Journal of Mechanical Sciences, **46(3)**, 411-431 **(2004)**.
- [19] Wetherhold, C.Robert, Singh, Aldraihem, J.Osama Tarunraj; Journal of Intelligent Material Systems and Structures, **8(2)**, 149-157 **(1997)**.
- [20] Lien-Wen Chen, Chung-Yi Lin, Ching-Cheng Wang; Composite Structures, **56**, 97-109 **(2002)**.
- [21] B.Ellad Tadmor, Gabor Kosa; Journal of Microelectromechanical Systems, **12(6)**, 899-906 **(2003)**.
- [22] N.Brij Agrawal, E.Kirk Treanor; Smart Materials Structures, **8**, 729-740 **(1999)**.
- [23] N.Christian Della, Dongwei Shu; Smart Mater.Struct., **15**, 529-537 **(2006)**.
- [24] M.Arafa, A.Baz; Composites: Part B, **31**, 255-264 **(2000)**.
- [25] Paolo Gaudenzi, Rolando Carbonaro, Edoardo Benzi; 'Control of Beam Vibrations by Means of Piezoelectric Devices', Theory and Experiments Composite Structures, **50**, 373-379 **(2000)**.
- [26] 26-http://www.efunda.com/materials/piezo/piezo_math/math_index.cfm, accessed in April, **(2006)**.
- [27] Chen Chang-Qing, Wang Xiao-ming, Shen Ya-peng; Journal of Computers & Structures, **60(3)**, 505-512 **(1996)**.
- [28] S.Narayanan, V.Balamurugan; Journal of Sound and Vibration, **262**, 529-562 **(2003)**.
- [29] S.S.Rao; 'Mechanical Vibrations', N.J. Upper Saddle River, Pearson Education 30-Daniel J.Inman, Engineering Vibration, Englewood Cliffs, N.J, Prentice Hall (1996) & **(2004)**.